L. E. (1980) *Science (Washington, D.C.) 208*, 1454-1457.
Reynolds, J. A., & Karlin, A. (1978) *Biochemistry 17*, 2035-2038.
Tzartos, S. J., & Lindstrom, J. M. (1980) *Proc. Natl. Acad. Sci. U.S.A. 77*, 755-759.
Tzartos, S. J., & Lindstrom, J. M. (1981) in *Monoclonal Antibodies in Endocrine Research* (Fellows, R., & Eisenbarth, G., Eds.) pp 69-86, Raven Press, New York.
Tzartos, S. J., Rand, D. E., Einarson, B. L., & Linstrom, J. M. (1981) *J. Biol. Chem. 256*, 8635-8645.
Tzartos, S. J., Seybold, M. E., & Lindstrom, J. M. (1982) *Proc. Natl. Acad. Sci. U.S.A. 79*, 188-192.
Walter, G., & Werchau, H. (1982) *J. Cell. Biochem. 19*, 119-125.

Kinetics of Divalent Cation Induced Fusion of Phosphatidylserine Vesicles: Correlation between Fusogenic Capacities and Binding Affinities†

Joe Bentz,* Nejat Düzgüneş, and Shlomo Nir

ABSTRACT: Fusion and aggregation of sonicated phosphatidylserine small unilamellar vesicles (PS SUV) induced by the divalent cations Ba^{2+}, Ca^{2+}, Sr^{2+}, and Mg^{2+} are studied and correlated with cation binding. Fusion is monitored with the terbium/dipicolinic acid (Tb/DPA) assay, which is supplemented by measuring the dissociation of preencapsulated Tb/DPA complex due to leakage of contents and entry of medium into the vesicles. The separate contributions of aggregation and fusion rates to the overall kinetics of membrane fusion are analyzed. In the presence of Na^+ or Li^+ concentrations of 300 mM or less, the rate of the overall fusion reaction induced by the divalent cations decreases in the sequence $Ba^{2+} > Ca^{2+} > Sr^{2+} > Mg^{2+}$ with respect to bulk concentrations. Under these conditions, both aggregation kinetics and bilayer destabilization are shown to affect the overall rate of fusion. In the presence of 500 mM Na^+ or Li^+ and subfusogenic concentrations of each of the divalent cations, the PS SUV reversibly aggregate; thus, the effect of the divalent cations (at larger, fusing concentrations) on the rate of bilayer destabilization can be examined directly. Here, Ba^{2+} and Ca^{2+} appear to be equally effective at inducing fusion. However, when the rate constant of fusion (which can be easily obtained in these cases) is compared with the amount of divalent cation bound per PS (calculated from binding constants which apply to the vesicles before aggregation and fusion), the fusogenic capacities of these divalent cations follow the sequence $Ca^{2+} > Ba^{2+} > Sr^{2+} > Mg^{2+}$.

The fusion of acidic phospholipid vesicles provides a basic model for biological membrane fusion in that there are three distinct, kinetically coupled stages common to both systems. First, the close apposition of bilayers is obtained by the aggregation of two or more vesicles. Second, the closely apposed bilayers must undergo a destabilization leading to an initial merging of the bilayers. Third, the merged bilayers must re-form into a continuous bilayer which encapsulates the mixed contents of each vesicle. Hence, we can use the vesicle systems to develop the biophysical theory required to examine the molecular mechanisms of membrane fusion. [See Nir et al. (1983) and Düzgüneş & Papahadjopoulos (1983) for reviews on phospholipid vesicle fusion.]

While there are many methods of monitoring fusion (Papahadjopoulos et al., 1974, 1976; Hoekstra et al., 1979; Liao & Prestegard, 1980a,b; Schullery et al., 1980; Schmidt et al., 1981; Vistnes & Puskin, 1981), those methods employing resonance or exchange energy transfer between fluorescent molecules are well suited for continuously monitoring the mixing of vesicle contents and bilayers (Struck et al., 1981; Wilschut & Papahadjopoulos, 1979). The terbium/dipicolinic acid (Tb/DPA)[1] assay (Wilschut et al., 1980, 1981), which measures the mixing of vesicle contents via the enhancement of Tb^{3+} fluorescence following chelation by DPA, is particularly suitable as the measured Tb fluorescence can be directly related to the number of fused vesicles (Nir et al., 1980b). The assay is sufficiently sensitive to allow the use of low vesicle concentrations, which is essential to examine the initial interaction of two vesicles. We have used this assay to determine both aggregation and fusion rate constants for PS SUV and LUV in Ca^{2+} (Nir et al., 1982; Bentz et al., 1983).

Here we will use the assay to quantitate the fusion kinetics of PS SUV induced by Ba^{2+}, Ca^{2+}, Sr^{2+}, Mg^{2+} in media containing either Na^+ or Li^+. We have introduced a new element to this assay: the dissociation of preencapsulated Tb/DPA complex which is due to both the leakage of complex into the medium and the influx of divalent cations and EDTA into the vesicles. This natural complement to the fusion assay is necessary because the fusion of PS SUV is somewhat leaky (Wilschut et al., 1980), and it is known that with Ca^{2+} the vesicles eventually transform into collapsed anhydrous structures (cochelates; Papahadjopoulos et al., 1975) which is the final equilibrium state. As models for biological membrane

† From the Departments of Pharmacy and Pharmaceutical Chemistry, School of Pharmacy (J.B.), and the Cancer Research Institute and Department of Anesthesia, School of Medicine (N.D.), University of California, San Francisco, California 94143, the Bruce Lyon Memorial Research Laboratory, Children's Hospital Medical Center, Oakland, California 94609 (N.D.), and The Seagram Centre for Soil and Water Sciences, Faculty of Agriculture, Hebrew University of Jerusalem, Rehovot, Israel (S.N.). *Received December 20, 1982.* This investigation was supported by Research Grants GM-31506 (J.B. and S.N.) and GM-28117 (N.D.) from the National Institutes of Health and Grant 1-768 from the March of Dimes Foundation (N.D.).

[1] Abbreviations: DPA, dipicolinic acid; EDTA, ethylenediaminetetraacetate; LUV, large unilamellar vesicle(s) (diameter ~100 nm); MLV, multilamellar vesicle(s); PC, phosphatidylcholine; PE, phosphatidylethanolamine; PS, phosphatidylserine; SUV, small unilamellar vesicle(s) (diameter ~30 nm); Tes, *N*-[tris(hydroxymethyl)methyl]-2-aminoethanesulfonic acid; EGTA, ethylene glycol bis(β-aminoethyl ether)-*N*,*N*,*N*′,*N*′-tetraacetic acid; TMA^+, tetramethylammonium.

0006-2960/83/0422-3320$01.50/0 © 1983 American Chemical Society

fusion, it is the initial events of vesicle fusion which are of primary importance, and the Tb/DPA assay provides a clear measure of these events.

With high monovalent cation concentrations, it is possible to make aggregation of the vesicles very rapid compared to the bilayer destabilization step; hence, the fusion assay is used to monitor the initial kinetics of the fusion step, per se, which mainly reflect the destabilization of the bilayers. Our results quantitate an earlier proposal that there is a critical amount of bound divalent cation necessary for the onset of PS bilayer destabilization (Nir et al., 1980a; Düzgüneş et al., 1981a). In addition, however, we show that each of the divalent cations studied has a different fusogenic capacity which correlates well with the effectiveness of these cations to affect equilibrium properties, including their ability to increase the gel to liquid-crystalline phase transition temperature of PS bilayers (Düzgüneş et al., 1981c) and to induce lateral phase separation in PS/PC bilayers (Ohnishi & Ito, 1974).

This study also elaborates on the questions of divalent cation binding to PS vesicles and the subsequent aggregation of the vesicles. It is shown that the different sets of cation binding constants which have been reported for various phospholipid membrane systems (Nir et al., 1978; Portis et al., 1979; McLaughlin et al., 1981; Ohki & Kurland, 1981) predict essentially identical amounts of bound divalent cations. We note, however, that these values pertain only to isolated membranes (before aggregation and fusion), since under conditions of fusion it appears that at least Ca^{2+} is capable of forming new, stronger binding complexes involving the apposed bilayers (Portis et al., 1979; Ekerdt & Papahadjopoulos, 1982). Our results allow a reexamination of the induction of aggregation of PS SUV by divalent cations (Ohki et al., 1982).

Materials and Methods

Phosphatidylserine from bovine brain was purchased from Avanti Polar Lipids (Birmingham, AL) and stored as a chloroform solution under argon at −40 °C. $TbCl_3$ was obtained from Alfa (Danvers, MA); dipicolinic acid (DPA, 2,6-pyridinedicarboxylic acid), Tes, L-histidine, and LiCl were from Sigma; NaCl was from Mallinckrodt (Paris, KY); $CaCl_2$, $BaCl_2$, $SrCl_2$, and $MgCl_2$ were from Fisher. Water was distilled twice, the second time in an all-glass apparatus.

Small unilamellar vesicles were prepared by sonication as described by Düzgüneş et al. (1981a) and contained either (i) 15 mM $TbCl_3$ and 150 mM sodium citrate, (ii) 150 mM DPA (Na salt), or (iii) 7.5 mM $TbCl_3$, 75 mM citrate, and 75 mM DPA. All solutions were buffered with 2 mM Tes and 2 mM L-histidine, pH 7.4. Unencapsulated material was eliminated by gel filtration on Sephadex G-75 (Pharmacia) by using 100 mM NaCl, 2 mM Tes, 2 mM L-histidine, pH 7.4 (NaCl buffer), and 1 mM EDTA as elution buffer. For calibration of the fusion assay, a portion of the Tb vesicles (type i above) was passed through another Sephadex G-75 column equilibrated with NaCl buffer (containing no EDTA). Vesicle concentrations were determined by phosphate analysis (Bartlett, 1959).

The Tb fluorescence scale was calibrated by lysing 25 μM Tb vesicles (freed of EDTA) with 0.5% (w/v) sodium cholate in the presence of 20 μM free DPA and sonicating for 5 min under argon in a bath-type sonicator. The fluorescence value obtained was set to 100%. As expected, 50 μM Tb/DPA vesicles (type iii above) gave 100% fluorescence by this calibration. Fluorescence and 90° light scattering measurements were made in an SLM 4000 fluorometer which allows simultaneous monitoring of fluorescence (excitation at 276 nm; emission at 545 nm, with a Corning 3-68 cutoff filter to eliminate contribution to the signal from light scattering, which was always less than 1.5% of the maximal Tb fluorescence intensity) and light scattering (using a Corning 7-54 band-pass filter). The output of the fluorometer was recorded on an Omniscribe chart recorder, at fast chart speeds when necessary. Additional details of the fusion assay have been described elsewhere (Wilschut et al., 1980).

The chelation of Tb and DPA is prevented outside the vesicles by the presence of the divalent cations and EDTA. In the case of Mg^{2+}-induced fusion, 0.1 mM EGTA was included in the medium in addition to the EDTA to enhance the quenching of the Tb fluorescence (Wilschut et al., 1981). Ba^{2+} and Sr^{2+} are also very effective in quenching Tb fluorescence in the presence of 0.1 mM EDTA as described below. The Tb/DPA complex which forms during the fusion of Tb and DPA vesicles will then be completely dissociated if it is released into the medium containing divalent cations and EDTA or if the medium enters the vesicle interior. The dissociation was measured directly by encapsulating the Tb/DPA complex and following the decrease in fluorescence (initially set at 100%) when fusion was induced by divalent cations.

When Tb/DPA complex is released during the fusion process, there is clearly a period of time, however small, where the complex resides outside of the vesicles but has not yet been fully diluted into the medium, where we know it will be dissociated completely. There are several lines of reason which show that during the initial stages of fusion studied here, this time period is negligibly small; i.e., the observed Tb fluorescence derives solely from Tb/DPA complex sequestered within the fused vesicles. Wilschut et al. (1980) showed during the initial stages of Ca^{2+}-induced fusion of PS SUV and LUV that the Tb fluorescence intensities could be fixed completely by the addition of excess EDTA. Thus, all of the Tb/DPA complex which had leaked into the medium had already been dissociated before the addition of excess EDTA. Now, it is possible to imagine that the extravesicular space within larger aggregates of vesicles would protect the released Tb, DPA, or Tb/DPA from a rapid dilution into the medium. During the initial stage of fusion, this possibility, which is the only way the Tb/DPA complex could survive outside of the vesicle interiors, is not supported by, and in fact is contradictory to, the available data. First, Bentz et al. (1983) have shown for PS SUV (2 mM Ca^{2+} and 100 mM Na^+) and PS LUV (5 mM Ca^{2+} and 100 mM Na^+) that virtually all of the Tb fluorescence is initially due to the fusion of dimer and trimer aggregates; i.e., essentially no larger aggregates have even formed. Obviously, dimers and trimers do not have any real extravesicular space which is protected from the medium, and all of the observed fluorescence must emanate from inside the fused vesicles. Second, we show here that when the Tb/DPA complex is preencapsulated into the vesicles and we monitor the dissociation of complex following fusion under conditions of rapid aggregation, i.e., in high monovalent cation concentrations, the dissociation is initially negligible, whereas after this latent period and when even larger aggregation products have formed the dissociation of complex is rapid and proceeds to completion. Thus, even in the larger aggregation–fusion products there is sufficient communication between the extravesicular space and the bulk medium to completely dissociate the Tb/DPA complex.

The *fusion experiment* starts with 25 μM each of Tb vesicles (type i above) and DPA vesicles (type ii above) and measures the kinetics of mixing of the vesicle contents during fusion.

The *dissociation experiment* starts with 50 μM Tb/DPA vesicles (type iii above) and measures the kinetics of Tb/DPA complex dissociation due to its leakage and the influx of divalent cations and EDTA into the vesicles during fusion. In fact, the fluorescence intensity measured at *any* time (either in the fusion experiment or in the dissociation experiment) equals the percentage of the total amount of Tb which is complexed with DPA at that time. With both types of experiments, the vesicles were suspended in 1 mL of NaCl buffer containing 0.1 mM EDTA in a quartz cuvette of 1-cm path length and stirred continuously at 25 °C. Divalent cations were added as a concentrated solution (20 mM to 1 M, depending on the final concentration to be achieved) with a Hamilton syringe.

Aggregation of vesicles was followed by (i) 90° light scattering at 276 nm as described above and (ii) absorbance at 350 nm in a Beckman Model 34 spectrophotometer by using quartz cells of 1-cm path length in a total volume of 1 mL.

Results

The Tb/DPA fusion assay has been described before (Wilschut et al., 1980, 1981; Düzgüneş et al., 1981a,b), and we use the same notation here. In a fusion experiment, the maximum fluorescence would be obtained if all of the encapsulated Tb were chelated by DPA, and the percent of maximal fluorescence for fusion (denoted % max *F*) is just the percent of encapsulated Tb which is complexed by DPA.

It is known that EDTA and Ca^{2+} will rapidly dissociate the Tb/DPA complex by competitive chelation, and the kinetics of this dissociation with Ca^{2+} are shown in Figure 2A of Wilschut et al. (1980). Similar kinetics are obtained for Mg^{2+} with 0.1 mM each of EDTA and EGTA, which were added to all Mg^{2+}-induced fusion experiments (Wilschut et al., 1981). We performed similar dissociation experiments with Ba^{2+} and Sr^{2+} and found that the dissociation kinetics were even faster than with Ca^{2+} (data not shown). For example, injecting 20 μL of 0.05 mM Tb^{3+}, 0.5 mM DPA^{2-}, and 0.5 mM citrate into 1 mL of 2.5 mM Ba^{2+}, 0.1 mM EDTA, and 100 mM Na^+ resulted in a 98% dissociation of the Tb/DPA complex within 3 s. This experiment roughly simulates the fluorescence kinetics which would follow from the instantaneous lysis of vesicles which contain the preformed Tb/DPA complex. Hence, during the divalent cation induced fusion experiments, the Tb fluorescence must come from the Tb/DPA complex inside of the fused vesicles, since any Tb/DPA released into the medium would be dissociated. On the other hand, the uptake of medium containing EDTA and divalent cations by the fusing vesicles would dissociate some of the Tb/DPA complex which had formed in the fused vesicles. We show here how to take this process into account.

Figure 1 shows the time course of the fusion of the PS SUV in 300 mM Na^+ and the various concentrations of divalent cations by the curves marked F. The control experiments (denoted as the dissociation experiment) were to encapsulate preformed Tb/DPA complex into the PS SUV and mix these vesicles with the same divalent cation concentrations. These results are shown by the curves marked D, where 0% max *D* implies that none of the Tb/DPA complex had dissociated and 100% max *D* means that all of the preformed complex has dissociated. It is clear that initially there is no dissociation of the Tb/DPA complex. On the other hand, over time, the dissociation curves clearly show a significant loss of Tb/DPA complex due to uptake of medium into and/or release of contents from the fused vesicles. The dissociation curves for 300 mM Li^+ and 500 mM Na^+ or Li^+ are similar and lead to the same conclusions.

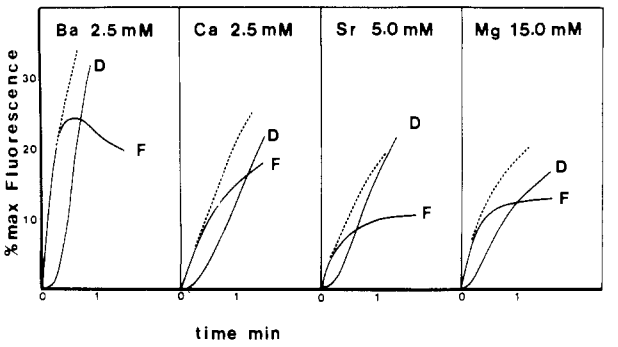

FIGURE 1: Fusion of PS SUV induced by each of the divalent cations in the presence of 300 mM Na^+ is shown over time. The fusion curve (F) is obtained from the mixing of Tb and DPA from separate PS SUV populations (25 μM concentration of each) and shows the percentage of encapsulated Tb which is complexed to DPA. The dissociation curve (D) is obtained from 50 μM PS SUV containing the Tb/DPA complex and shows the percentage of Tb/DPA complex which has dissociated due to the leakage from and entry of medium into the vesicles. The contribution to the observed fluorescence levels from scattered light is always less than 1.5% (see Materials and Methods for further details). The dotted line is the fusion curve F corrected for the loss of fluorescence due to dissociation as estimated by the sum of $F + 0.5D$ (see footnote 2). With 500 mM Na^+, or 300 or 500 mM Li^+, the curves are qualitatively the same.

The dotted lines in Figure 1 represent corrected fusion curves given by the sum of $F + 0.5D$, which initially is equal to the fluorescence which would be observed if there were no dissociation of complex following fusion.[2] These corrected curves show that the fusion continues in time and that the maximum in the F curves, seen especially with Ba^{2+}, is due to the dissociation of complex. Since the initial rate of Tb/DPA formation (i.e., the slope of the fusion curve F, with the units % max *F* per min) is negligibly affected by leakage of material either into or out of the fused vesicles, it is a proper measure for the initial rate of vesicle fusion. However, this initial rate embodies the kinetics of vesicle aggregation followed by the kinetics of bilayer destabilization.

In Figure 2, we show the 90° light scattering, in addition to the light absorbance, induced by *subfusogenic* concentrations of divalent cations in 500 mM Na^+. In 500 mM Na^+ or Li^+ alone, there is no aggregation of the vesicles, but their aggregation could be produced (without fusion or leakage) by the divalent cations. In Li^+, slightly higher divalent cation concentrations were required. This may be expected from studies on monovalent cations where more Li^+ than Na^+ is needed to induce the aggregation of vesicles (Ohki et al., 1982). From these data, we know that the onset of fusion at higher divalent cation concentrations is not rate limited by the aggregation step. In the next section, we will show how to extract

[2] A numerical example will clarify this point. Suppose that half of the vesicles have fused to doublets and the other half are either monomers or unfused dimers. If there were no dissociation, then $F = 25\%$, since only half of the fused doublets will contain the Tb/DPA complex while the other half contains only Tb or DPA. On the other hand, if 20% of the complex which formed has subsequently dissociated, due to leakage and medium uptake, then $F = 20\%$. In this case, the dissociation experiment will show $D = 10\%$; i.e., in the vesicles which have undergone fusion (50%), there will be 20% dissociation of the preencapsulated complex. Therefore, $F + 0.5D = 20\% + 0.5(10\%) = 25\%$, i.e., the same amount expected if there were no dissociation. When there are higher order fusion products (fused triplets etc.), *D* must be multiplied by a factor between 0.5 and 1 [as explained in Nir et al. (1980b) and Bentz et al. (1983)] in order to estimate the amount of fluorescence which is lost due to dissociation. Here we will use $0.5D + F$ as a simple underestimate of the amount of fluorescence expected if there were no dissociation of the complex.

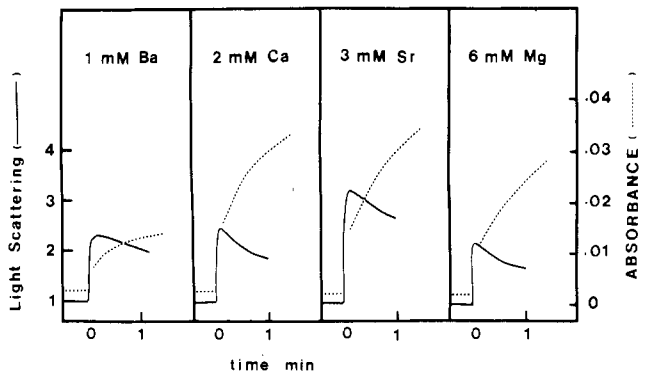

FIGURE 2: Aggregation over time of the PS SUV in 500 mM Na^+ and the indicated concentration of divalent cation is shown both by 90° light scattering (276 nm) with the solid line and by light absorbance (350 nm) with the dotted line. Before addition of the divalent cation (at $t = 0$), the vesicles are dispersed and the light scattering intensity is normalized to 1, while the light absorbance (shown in optical density units) is 0.002. After addition of the divalent cation, there is no measurable fusion or dissociation (data not shown). The light scattered or absorbed by the salt solutions alone is negligible on the scale shown. The light absorbance at 450 nm is less than that at 350 nm, but otherwise, the curves are similar. The subsequent fall in scattered light intensities is due to interference effects, which have a much smaller effect on the light absorbance as shown by its continued increase in time (see text).

fusion rate constants from these data, where the aggregation is clearly rapid.

The light-scattering curves also show that 90° light scattering, while a measure of the existence of aggregation, cannot be used generally to quantitate aggregation. The decrease in the magnitude of scattered light is due to the fact that the aggregates are becoming sufficiently large (compared with the light's wavelength) such that interference effects reduce the intensity of scattered light (Kerker, 1969; Bentz & Nir, 1981a; Nir et al., 1981). In fact, large unilamellar vesicles (LUV, diameter ~0.1 μm) are even more susceptible to these interference effects, sometimes yielding only decreases in the relative scattered light (Sundler & Papahadjopoulos, 1981; Düzgüneş, et al., 1981b). Light absorbance, however, is less sensitive to interference effects, since it is the low-angle scattering which contributes most to this parameter (Kerker, 1969). Thus, the absorbance increases following aggregation. (See dotted curves in Figure 2.)

Figure 3a shows the initial rates of fusion (as % max F per min) vs. Ca^{2+} bulk concentration for a variety of Na^+ concentrations. For a given Na^+ concentration, the initial fusion rate increases with Ca^{2+} concentration. From Figure 2, we know that in 500 mM Na^+ the fusion is rate limited by the destabilization step, since aggregation occurs readily at or above 2 mM Ca^{2+}. Previously, Nir et al. (1980b) showed that in 100 mM Na^+ with 1.25 and 1.5 mM Ca^+, the overall fusion was rate limited by aggregation. In the lower Na^+ concentration range (≤100 mM), the rate of the overall fusion process increases with Na^+ concentration provided that the Ca^{2+} concentration is above 1.25 mM. Since Na^+ itself does not cause bilayer destabilization and since increased Na^+ would only decrease the amount of bound Ca^{2+}, there would be no increase in the bilayer destabilization rate. Under these ionic conditions, the aggregation kinetics are dominating the initial kinetics of the overall fusion reaction. We note here that the initial Tb/DPA dissociation kinetics are not always negligible at the lower Na^+ concentrations; however, the correction is small in all cases.

The balance between the kinetics of aggregation and destabilization in this system is clarified considerably by knowing the amounts of Ca^{2+} bound per PS for each system. Figure 3b shows the calculated amounts of Ca^{2+} bound per PS vs. the bulk Ca^{2+} concentration for the same set of Na^+ con-

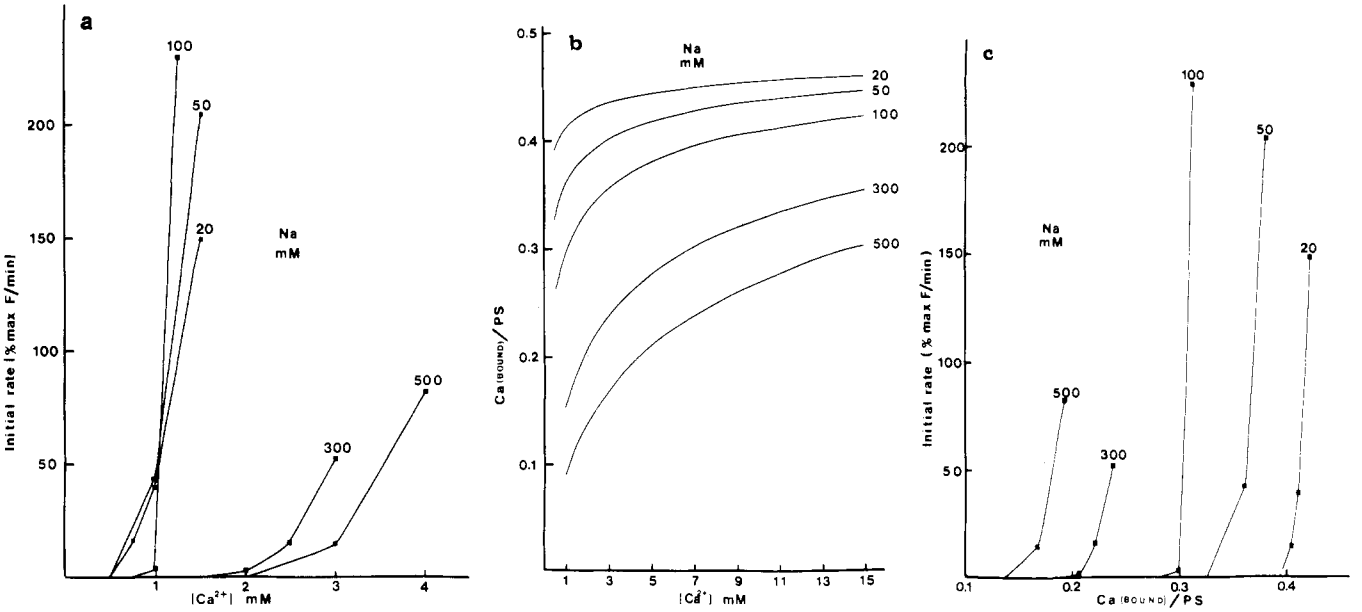

FIGURE 3: (a) Initial rate of fusion (defined as the initial slope of the F curve, as in Figure 1, in the units of % max F per min) is shown as a function of Ca^{2+} concentration for a variety of Na^+ concentrations. Since the initial dissociation is always negligible (see Figure 1), there is no need to correct the fusion curve for the loss of fluorescence due to complex dissociation. The data points are shown by the closed squares except at the points of zero initial fusion where the symbols are omitted for clarity. At these points, there was no measurable fusion or dissociation (<1% max F or D) for at least 2 min. (b) Calculated amount of Ca bound per PS is shown as a function of the bulk Ca^{2+} concentration with the same set of Na^+ bulk concentrations as in Figure 3a. The calculations pertain to isolated PS SUV, i.e., before the aggregation and fusion have begun. The binding constants of McLaughlin et al. (1981) were used: $K(Na) = 0.6\ M^{-1}$ and $K(Ca) = 12\ M^{-1}$ with Ca^{2+} binding to a single PS head group. The other details of the calculations are described in the footnote to Table IV and in the Appendix. The reduced Ca^{2+} binding with increasing Na^+ concentrations is due to the direct binding competition between the Na^+ and Ca^{2+} and to the reduction of the Ca^{2+} concentration near the vesicles' surface due to the increased ionic strength which reduces the surface potential of the vesicle (Bentz, 1981). (c) Initial rates of fusion (% max F per min) from Figure 3a are replotted here as a function of the calculated amount of bound Ca^{2+} per PS head group by using the curves of Figure 3b.

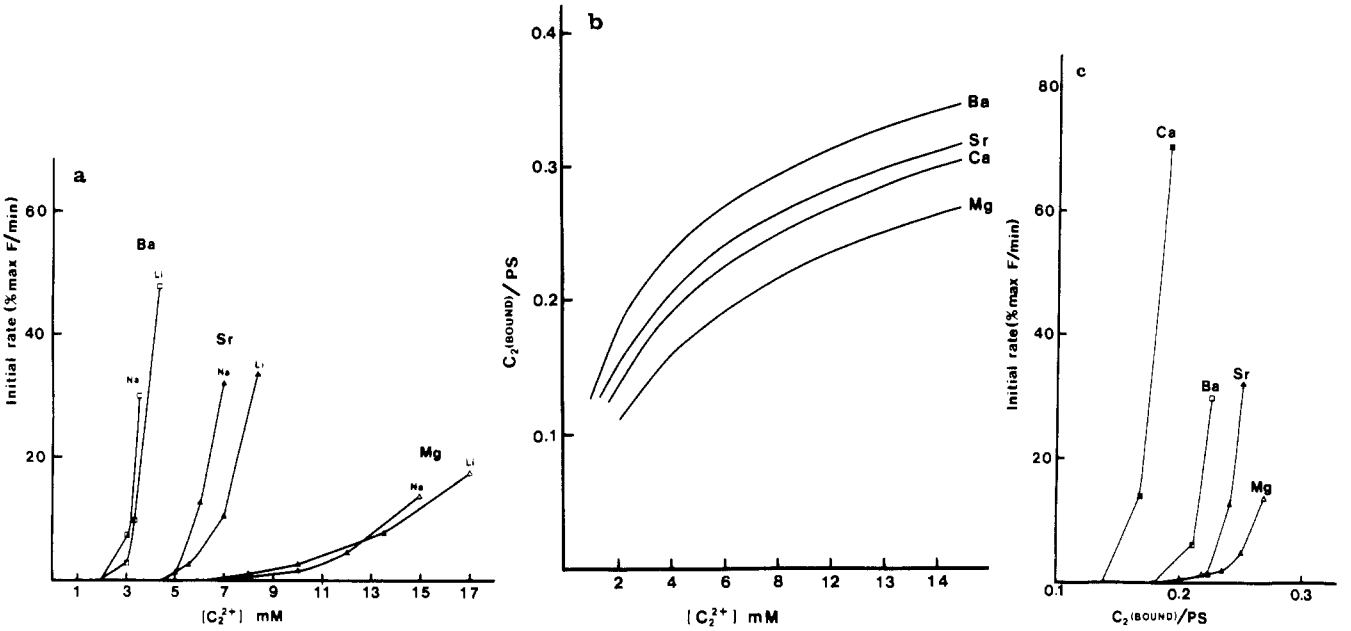

FIGURE 4: (a) Initial rates of fusion (% max F per min, from the initial slope of the F curves as in Figure 1) are plotted against the bulk concentration of the divalent cations Ba^{2+} (□), Sr^{2+} (▲), and Mg^{2+} (△) with 500 mM either of Na^+ or of Li^+ in the medium, as indicated. The curves for Ca^{2+} lie essentially on top of the Ba^{2+} curves and are omitted for clarity. In all cases, including Ca^{2+}, at the concentrations where the curves intersect the ordinate (zero initial fusion), there is substantial aggregation and no measurable fusion or dissociation (<1% max F or D) for at least 2 min. (b) Calculated amounts of divalent cation bound per PS for SUV are shown as a function of the bulk concentration of that divalent cation in 500 mM Na^+. The binding constants of McLaughlin et al. (1981) are used: $K(Ba) = 20\ M^{-1}$, $K(Sr) = 14\ M^{-1}$, $K(Ca) = 12\ M^{-1}$, and $K(Mg) = 8\ M^{-1}$. These binding constants were obtained by assuming that each of the cations can bind only to a single PS head group. Likewise, these calculations pertain only to the vesicles before aggregation and fusion have begun. See Figure 3b and the Appendix for more details. The corresponding curves for 500 mM Li^+ [with $K(Li) = 0.8\ M^{-1}$] are qualitatively the same, with slightly less bound divalent cation per PS at each bulk concentration. (c) Initial rates of fusion (% max F per min) from Figure 4a, including the data for Ca^{2+} (■), for 500 mM Na^+ are replotted here as a function of the calculated amounts of the divalent cation bound per PS by using the curves of Figure 4b. The corresponding curves for 500 mM Li^+ are qualitatively identical; see Table I.

centrations. (See text below and the Appendix for a discussion of these calculations.) Figure 3c shows the initial rates of fusion for these systems now plotted against the amount of Ca^{2+} bound per PS. It is evident from the 500 mM Na^+ curve that the amount of Ca^{2+} bound per PS needed to induce the destabilization of apposed bilayers is only about 0.15.[3] In 20 mM Na^+ and 0.5 mM Ca^{2+}, the vesicles have enough bound Ca^{2+} to fuse but are prevented from doing so because they cannot aggregate.

We can now extend this analysis to the other divalent cations, Ba^{2+}, Sr^{2+}, and Mg^{2+}. Figure 4a shows the initial rates of fusion for these cations with either 500 mM Na^+ or 500 mM Li^+. Recall from Figure 2 that aggregation occurs readily here even below the fusion thresholds. The curves for Ca^{2+} lie essentially on top of the Ba^{2+} curves and are omitted for clarity. Li^+ appears more inhibitory to fusion than Na^+, except for the case of Mg^{2+} where the initial rates are similar.

In order to relate these fusion rates to the bound cations, we show first, in Figure 4b, how the amounts of bound divalent cation vary with their bulk concentration in 500 mM Na^+. These values are calculated from the binding constants of McLaughlin et al. (1981); however, in the Appendix, we show that other proposed sets of divalent cation binding constants [e.g., see Nir et al. (1978), Portis et al. (1979), and Ohki & Kurland (1981)] yield essentially identical estimates for the amounts of bound Ca^{2+} and Mg^{2+}. As pointed out in footnote 3, these values for the bound divalent cation pertain only to isolated (nonaggregated) vesicles.

In the range of 2–4 mM divalent cation, where Ba^{2+}, Ca^{2+}, and Sr^{2+} all begin to induce rapid fusion, the amounts of bound divalent cations increase from 0.1 to 0.2. However, since the binding constant for Sr^{2+} ($14\ M^{-1}$) is larger than that for Ca^{2+} ($12\ M^{-1}$), there is more Sr^{2+} bound than Ca^{2+} at a given bulk concentration. Since 4 mM Ca^{2+} can induce fusion in 500 mM Na^+ or Li^+, while Sr^{2+} can induce only aggregation, it is clear that Ca^{2+} is more fusogenic than Sr^{2+}. In fact, the cations' relative capacities to induce fusion are clearly shown in Figure 4c where the initial rates of fusion are plotted against bound divalent cation. In either Na^+ or Li^+ (results for Li^+, which are similar to those for Na^+, are not shown), the fusogenic capacities are in the sequence $Ca^{2+} > Ba^{2+} > Sr^{2+} > Mg^{2+}$.

Discussion

The results show that each of the divalent cations Ba^{2+}, Ca^{2+}, Sr^{2+}, and Mg^{2+} can induce the fusion of PS SUV, as reported previously (Düzgüneş et al., 1981c; Ohki, 1982). With large Na^+ or Li^+ concentrations, the initial fusion does not involve any significant exchange between the encapsulated contents of the vesicles and the medium (Figure 1). In high Na^+ or Li^+ concentrations (>300 mM), the vesicles can be aggregated, without fusion or leakage, by small amounts of each of the divalent cations (Figure 2). The rate-limiting step for the overall fusion event can be the aggregation step, as it

[3] This and the other values of bound cation per PS are obtained from the binding constants shown in Table II and the equations described in the Appendix. The most important point to recognize for these calculations is that they are valid only for isolated (unaggregated) vesicles. When the vesicles aggregate, the amount of bound divalent cation will increase by 20–30% simply due to the close approach of the charged surfaces (Bentz, 1982). In addition, as discussed later, there is substantial evidence that during and/or after fusion there is a new, stronger binding complex between (at least) Ca^{2+} and the PS. Therefore, put more rigorously, this fusion threshold of 0.15 represents the amount of bound Ca per PS on the initially isolated vesicle which is necessary to produce the initial fusion rate threshold (10% max F per min), regardless of how the actual amount of bound Ca^{2+} changes during the subsequent aggregation and fusion processes.

Table I: Divalent Cation Concentrations and Divalent Cation Bound per PS at an Initial Fusion Rate Threshold of 10% max F/min[a]

	(A) bulk concn of divalent cation (mM) with			
	300 mM		500 mM	
	Li	Na	Li	Na
Ca	2.8	2.3	3.7	2.7
Ba	2.5	2.0	3.4	3.1
Sr	5.5	4.5	7.0	6.0
Mg	14.0	12.5	14.5	14.0
	(B) bound divalent cation (per PS) with			
	300 mM		500 mM	
	Li	Na	Li	Na
Ca	0.20	0.22	0.16	0.16
Ba	0.23	0.25	0.20	0.21
Sr	0.27	0.28	0.22	0.24
Mg	0.29	0.31	0.24	0.26

[a] The bulk concentration of divalent cation at the fusion threshold (defined as an initial rate of fusion of 10% max F/min) is obtained directly from Figure 4 and the corresponding data for Li^+. These values do not account for the 0.1 mM EDTA in the medium; hence, the true bulk concentrations are about 0.1 mM less. Otherwise, the uncertainty for these bulk concentrations is about ±0.1 mM. The calculated amounts of divalent cation bound per PS are obtained from the binding constants of Eisenberg et al. (1979) and McLaughlin et al. (1981) as described in Table III and in the Appendix. The experimental uncertainties in the values of these binding constants produce an uncertainty of about ±0.01 in these calculated values. These values pertain only to the vesicles before the fusion process begins; see footnote 3.

is in Na^+ or Li^+ concentrations at or below 100 mM, or it can be the bilayer destabilization itself, as it is when the Na^+ or Li^+ concentration is large (500 mM). As the Na^+ or Li^+ concentration is increased above 300 mM, progressively larger divalent cation concentrations are required to induce fusion (Figure 3a).

The essential results of our experiments and calculations are summarized in Table I where we have given the amounts of divalent cation, both present in bulk concentration and bound to the single vesicle, needed to induce a threshold initial fusion rate of 10% max F per min. We note that the bulk concentrations of divalent cations needed to induce threshold fusion in 300 mM Na^+ or Li^+ and in 500 mM Li^+ increase in the sequence $Ba^{2+} < Ca^{2+} < Sr^{2+} < Mg^{2+}$. However, in 500 mM Na^+, we find that Ca^{2+} is more effective in inducing fusion than Ba^{2+}.

In part B of Table I, we show the calculated amounts of bound divalent cation at these fusion thresholds, using the binding constants of McLaughlin et al. (1981). Here, we find that in all of the cases less Ca^{2+} is bound per PS than Ba^{2+}. To the extent that these binding constants are accurate (and in the Appendix we provide evidence from other studies to support these calculations for Ca^{2+} and Mg^{2+}), it appears that Ca^{2+} has a greater fusogenic capacity than does Ba^{2+}; i.e., less bound Ca^{2+} than Ba^{2+} is necessary initially to induce the bilayer destabilization.

Initial Stage of Fusion. We have introduced a mass action kinetic model of vesicle fusion (Nir et al., 1982; Bentz et al., 1983), the first step of which is

$$V_1 + V_1 \underset{D_{11}}{\overset{C_{11}}{\rightleftharpoons}} V_2 \xrightarrow{f_{11}} F_2 \qquad (1)$$

The aggregation of two single vesicles, V_1, to the unfused dimer, V_2, is governed by the kinetic rate constants for dimerization, C_{11}, and dissociation, D_{11}. The fusion of the dimer, yielding the fused doublet, F_2, is governed by the fusion rate constant, f_{11}. In order to understand the mechanism of vesicle fusion, and in fact the mechanism of fusion in cellular systems, it is necessary to separate the kinetics of aggregation from the kinetics of the fusion step itself. While it is possible to extract the values of each of the kinetic rate constants by analyzing the dependence of the overall fusion rates on vesicle concentration (Bentz et al., 1983), we have shown here that the kinetics of bilayer destabilization can be examined directly by producing aggregation kinetics which are sufficiently rapid. Below, we will show how some of the data given here can be translated directly into the values of f_{11}.

In particular, we note that for each divalent cation there is a threshold amount bound to the membrane, below which f_{11} is quite small and above which the value of f_{11} rises quickly (Figure 4c). The simplest conceptual model for the relationship between f_{11} and the amount of bound divalent cation is that f_{11} continues to increase with bound divalent cation until some maximum level is reached. At the lower Na^+ concentrations, the Ca^{2+}-induced aggregation is always accompanied by fusion since the amount of bound Ca^{2+} is large, whereas at the higher Na^+ concentrations, aggregation could be induced without fusion (Figure 2). At the Ca^{2+} concentrations where the initial fusion rates approach zero (Figure 3a), the amounts of bound Ca^{2+} in the lower Na^+ concentration cases are well above the fusion threshold for Ca^{2+} (Figure 3c); thus, the vesicles have sufficient bound Ca^{2+} to undergo fusion, but they do not aggregate due to their mutual electrostatic repulsion (Nir & Bentz, 1978; Nir et al., 1980a; Bentz & Nir, 1981a,b). The value of f_{11} may be large, but unless C_{11} is also large enough to promote sufficient aggregation, there will be no measurable fusion.

Divalent Cation Induced Aggregation. The previous discussion illustrates how the Tb/DPA fusion assay can be used also to measure aggregation rates (in ionic conditions which induce vesicle fusion) separately from bilayer destabilization rates (f_{11}). This property was exploited (Nir et al., 1980b) to measure the C_{11} values for PS SUV in 100 mM Na^+ and 1.25 and 1.5 mM Ca^{2+}. From our previous results, together with those shown here, we find that C_{11} increases with the amount of bound cation (as the vesicles' surfaces become increasingly neutralized by the bound divalent and monovalent cations), and f_{11} increases with the amount of bound divalent cation in the sequence $Ca^{2+} > Ba^{2+} > Sr^{2+} > Mg^{2+}$. However, the effect of cation binding on the dissociation rate constant D_{11} is unknown. Previous work has shown that aggregation increases with the value of $C_{11}[X_0]/D_{11}$, where $[X_0]$ is the initial vesicle concentration (Bentz & Nir, 1981a,b). Thus, measurable aggregation will occur only if D_{11} is sufficiently small.

Recently, Ohki et al. (1982) determined with light absorbance that PS SUV in 100 mM Na^+ could be induced to aggregate by divalent cations with a sequence of effectiveness decreasing in the sequence $Ba^{2+} > Ca^{2+} > Sr^{2+} > Mg^{2+}$, i.e., the same sequence we found in the lower Na^+ concentrations where aggregation is completely rate limiting to the overall fusion. They showed also that the monovalent cations alone could induce reversible aggregation in the sequence $Na^+ > Li^+ > K^+ > TMA^+$. The same sequence has been found by dynamic light scattering (J. Ho, personal communication). These sequences differ somewhat from the binding constant sequences obtained by Eisenberg et al. (1979) and McLaughlin et al. (1981), who found that the order of binding constants was $Sr^{2+} > Ca^{2+}$ and $Li^+ > Na^+$ by electrophoretic mobility measurements.

Table II: Fusion in 500 mM Na^+

(A) Percent of Maximal Fluorescence[a]

	3.5 mM Ba^{2+}		3.0 mM Ca^{2+}		6.0 mM Sr^{2+}		15.0 mM Mg^{2+}	
t (s)	exptl[b]	theor[b]	exptl	theor	exptl	theor	exptl	theor
5	2.5	3.1	1.0	1.5	0.9	1.2	1.2	1.5
10	5.3	6.1	2.3	2.9	2.0	2.4	2.5	2.9
15	8.1	8.9	3.8	4.3	3.5	3.6	3.9	4.3
30	17.0	16.1	8.5	8.2	7.4	7.0	8.2	8.2
45	25.5	22.1	12.0	11.8	10.1	10.1	12.1	11.8
60	30.6	27.1	15.3	15.1	12.7	13.0	16.2	15.1

(B) f_{11} Values[c]

	f_{11}(fitted) (s^{-1})	f_{11}(initial rate) (s^{-1})
3.5 mM Ba^{2+}	0.013	0.01
3.0 mM Ca^{2+}	0.006	0.005
6.0 mM Sr^{2+}	0.005	0.004
15.0 mM Mg^{2+}	0.006	0.0045

[a] Corrected for dissociation, $F + {}^1/_2D$, vs. theoretically predicted values, $I(t)$, from eq 4. [b] The experimental values are $F + {}^1/_2D$ from the equivalent data as shown in Figure 1. The theoretical values are $I \times 100$ by using eq 4 with the f_{11} values shown in Table IIB in the column labeled f_{11}(fitted). [c] Obtained from the fit over time, f_{11}(fitted), from Table IIA vs. the values estimated from the initial rate of fusion, f_{11}(initial rate), from eq 5.

We have confirmed the finding of Ohki et al. (1982) that Ca^{2+} is also more effective than Sr^{2+} in inducing just aggregation by using a system where there is no fusion of the PS SUV. In 500 mM Na^+, the light absorbance due to 2 mM Ca^{2+} (Figure 2) was about 2 times greater than that produced by 2 mM Sr^{2+} (data are similar to those for 1 mM Ba^{2+}). Thus, we would speculate that Sr^{2+} induces a more reversible aggregation than Ca^{2+} and that it is this effect which underlines the difference between the binding and aggregation sequences. Also germane to this point is the observation that reversibility is negligible for fusion of PS LUV (diameter ~0.1 μm) induced in 100 mM Na^+ and 5 mM Ca^{2+} (Bentz et al., 1983). Sr^{2+} can induce fusion of the PS LUV, but only at large bulk concentrations (Düzgüneş et al., 1983a); i.e., the capacity of Sr^{2+} to induce the fusion of PS LUV is much reduced compared with Ca^{2+} and Ba^{2+}. Furthermore, it is known that Mg^{2+} cannot induce the fusion of these PS LUV (Wilschut et al., 1981), whereas their reversible aggregation does occur (Nir et al., 1981). Although further quantitative data will be needed, taken together, these facts support the hypothesis that the aggregation induced by Sr^{2+} is more reversible than that produced by Ca^{2+} and that the molecular mechanism responsible for this reversibility may be related to the vesicle size dependence of the divalent cations' fusogenic capacities.

Fusion Rate Constants. The value of the fusion rate constant (f_{11}) is a direct measure of the molecular mechanism of membrane fusion. Here, we will show how to extract the value of f_{11} when the aggregation of the vesicles is rapid compared with their subsequent fusion, i.e., in 500 mM Na^+ or Li^+.

If we presume that all of the vesicles dimerized and then began to fuse, the appropriate initial mass action reaction would be

$$V_2 \xrightarrow{f_{11}} F_2 \qquad (2)$$

The initial concentration of dimers can be given by $[V_2(0)] = {}^1/_2[X_0]$ where $[X_0]$ denotes the initial concentration of vesicles. When only reaction 2 is occurring, which would be true initially, the concentration of fused doublets $[F_2]$ is given by

$$\frac{[F_2]}{[X_0]} = {}^1/_2[1 - \exp(-f_{11}t)] \qquad (3)$$

When there are only fused doublets, then the expected *fraction* of maximal Tb fluorescence [corrected for dissociation, i.e., $I(t) = (F + {}^1/_2D)/100$] is (Bentz et al., 1983; Nir et al., 1982)

$$I(t) = \frac{[F_2]}{[X_0]} = {}^1/_2[1 - \exp(-f_{11}t)] \qquad (4)$$

as explained in footnote 2. When there are higher order aggregates (less than or equal to tetramers), then it can be shown that essentially the same expression for $I(t)$ is obtained at early times. Hence, when the aggregation is rapid compared with fusion, we can estimate f_{11} directly.

In Table IIA, we show the fit from eq 4 to the data for fusion induced by the divalent cations in 500 mM Na^+. Since the aggregation of the vesicles must always occur first, we expect eq 4 to first overestimate the observed (corrected) fluorescence. Likewise, as higher order fusion products form, we expect eq 4 to underestimate the experimental values. The results of Table IIA are consistent with these expectations. The values of f_{11} used to fit these data are given in Table IIB under the column labeled f_{11}(fitted).

Using eq 4, we can also estimate f_{11} from the data presented in Figure 4. The initial slope of I is $(d/dt)I\ (t = 0) = {}^1/_2f_{11}$, and it equals the initial rate of fusion, i.e., % max F per min divided by 6000 to convert the units to the fraction of maximal fluorescence per second. Thus, the data of Figure 4 give direct estimates for f_{11} as

$$f_{11}(\text{initial rate}) = (\%\ \text{max}\ F/\text{min}) \div 3000\ (s^{-1}) \qquad (5)$$

Table IIB shows these estimates for f_{11}, under the column labeled f_{11}(initial rate), for the cases given in Table IIA. The concordance between the estimates for f_{11} by using just the initial fusion rates and fitting the whole curve is good. The fact that eq 4 ignores the initial aggregation step accounts for the fact that f_{11}(initial rate) is slightly less than f_{11}(fitted).

In Table I, we showed the amounts of divalent cations bound needed to produce 10% max F per min as an initial fusion rate, which from eq 5 implies $f_{11} \simeq 0.0033\ s^{-1}$. From eq 3, we see that with this fusion rate constant about 10% of the vesicle dimers have fused in 30 s. This fusion rate constant, being right at the threshold for fusion, is small. By way of comparison, we have shown that PS SUV in 100 mM Na^+ and 2 mM Ca^{2+} have a fusion rate constant $f_{11} \simeq 5\ s^{-1}$ (Nir et al., 1982; Bentz et al., 1983). This would give a 10% fusion of preaggregated dimers in ~20 ms. Miller & Dahl (1982) have corroborated that prediction with rapid freeze fracture

by showing the fusion of PS SUV in 10 mM Ca^{2+} at 10 ms, which is the limit of time resolution for their experimental system. From Figure 4, it is evident that the fusion rate constant is extremely sensitive to the identity and the amount of bound divalent cation.

It is of interest to compare the very rapid aggregation and fusion of PS SUV where dimers can form and fuse in seconds or less with the quite slow aggregation and fusion of DPPC SUV which occur on the order of hours to weeks (Wong et al., 1982). Wong & Thompson (1982) proposed a model in which the reactions leading to fusion require substantial preaggregation of the DPPC vesicles, suggesting a rather different fusion mechanism from that operating with divalent cation induced fusion of PS vesicles which begins with dimers.

Fusogenic Capacity vs. Divalent Cation Binding. We have relied on the binding constants of the cations to the exterior surface of PS MLV derived from microelectrophoresis (Eisenberg et al., 1979; McLaughlin et al., 1981) in order to quantitate the relationship between divalent cation bound to the isolated vesicle and the initial rates of fusion. In the Appendix, we have shown that for Na^+, Ca^{2+}, and Mg^{2+} the results of other binding studies (Newton et al., 1978; Nir et al., 1978; Portis et al., 1979; Kurland et al., 1979; Düzgüneş et al., 1981a; Ohki & Kurland, 1981) yield essentially the same calculated values of bound divalent cation, although the values of other parameters, e.g., surface charge densities and amounts of bound monovalent cations, are different. This concordance between the various binding studies, for the amount of bound divalent cation, indicates that the different geometries of the PS membranes used (SUV, LUV, MLV, and monolayer) do not significantly affect the binding of the cations to the PS head groups. As discussed in the Appendix, other types of binding models are conceivable, and new binding studies will be necessary to determine the correct binding model. However, it is now evident that the amounts of bound divalent cation can be reliably predicted, and the sequence of fusogenic capacities is established.

The binding of divalent cations to isolated PS surfaces (as reflected by the binding constants) is clearly distinguished from their subsequent ability to induce the fusion of the vesicles (as reflected by their fusogenic capacities). The probable cause of this difference is given in recent studies by Rehfeld et al. (1981) and Ekerdt & Papahadjopoulos (1982). Their results show that the amount of bound Ca^{2+} markedly increases with vesicle aggregation and fusion. While it is expected that the amount of bound Ca^{2+} will increase when the vesicles aggregate (by about 20–30%; Bentz, 1982), the extent of the measured increase greatly exceeded these predicted amounts. This would indicate the emergence of a new binding complex due to or following the fusion of the vesicles. This new binding complex is proposed to involve the apposed head groups of the PS molecules being bridged by Ca^{2+} (Portis et al., 1979; Ekerdt & Papahadjopoulos, 1982). We have found also that in 900 mM Na^+ or Li^+, where the vesicles are preaggregated, injection of 2 mM Ca^{2+} will induce very slow fusion although the calculated amounts of bound Ca^{2+} to isolated vesicles are quite small (<0.074 and 0.057, respectively; see Table IV). The emergence of new binding complexes following vesicle fusion has also been found with the trivalent cation La^{3+} (Hammoudah et al., 1981). However, it has not yet been shown that these binding complexes exist coincident with the onset of fusion.

The evidence that new binding complexes also emerge for the other divalent cations is more circumstantial, but none the less compelling. Ohnishi & Ito (1974) showed that the extent of the phase separations induced by the divalent cations decreased in the same sequence as that of their fusogenic capacities observed in this study, i.e., $Ca^{2+} > Ba^{2+} > Sr^{2+} \gg Mg^{2+}$. However, Hoekstra (1982a,b) concluded that the rate of fusion of PS/PC SUV in the presence of Ca^{2+} is faster than the rate of phase separation, whereas for the PS/cholesterol SUV these two processes occur at about the same rate. Furthermore, the fusion of PS/PE (1:3) LUV in both Ca^{2+} and Ca^{2+}/Mg^{2+} mixtures exhibits an acceleration in the fusion of the vesicles after about a minute (Düzgüneş et al., 1981b) which corresponds to the time required for significant phase separation in PS/PC membranes (Hoekstra, 1982a,b).

If the lateral phase separation is driven by the formation of the new binding complexes, then we would expect these results; i.e., the kinetics of the two processes are coupled, but they need not be identical. At present, there is no evidence which specifies whether the lateral phase separation can occur on isolated vesicles or whether, like the new binding complexes, it requires the apposition of another bilayer.

The other major phenomenon attributed to the emergence of new binding complexes is the extent to which divalent cations shift the gel to liquid-crystalline phase transition temperature (T_c) of brain PS bilayers (relative to the T_c in 100 mM Na^+ buffer alone) which decreases in the same sequence, i.e., $Ca^{2+} > Ba^{2+} > Sr^{2+} > Mg^{2+}$ (Düzgüneş et al., 1981c). This sequence is obtained both for PS LUV mixed with the divalent cations (N. Düzgüneş and J. Paiement, unpublished results) and for PS MLV formed in the divalent cations. It is known that Ba^{2+} and Sr^{2+} will induce the fusion of PS LUV at temperatures above the T_c of the metal ion/PS complex (Düzgüneş et al., 1983b), which implies that the isothermal phase transition induced by these cations is not required for fusion. However, using titration microcalorimetry, it has been shown that there is a small endothermic reaction at 25 °C induced by the binding of the divalent cations to the isolated PS SUV and, more importantly, a large exothermic reaction once the vesicles begin to aggregate and fuse (Düzgüneş et al., 1981c). The magnitude of this exothermic reaction decreases in the sequence $Ca^{2+} > Ba^{2+} > Sr^{2+} > Mg^{2+}$. This clearly implies the emergence of new binding complexes following the apposition of the bilayers.

It has been proposed that the extent of dehydration of the PS head groups due to divalent cation binding is related to the initiation of bilayer destabilization (Portis et al., 1979; Ohki & Düzgüneş, 1979; Wilschut et al., 1981; Hoekstra, 1982b; Düzgüneş & Papahadjopoulos, 1983). It is known that the MLV formed in Ca^{2+} contain essentially no water between the bilayers (which is the proposed reason for the very high value of T_c), whereas in Mg^{2+} the bilayers are separated by a layer of water ~7 Å thick (Portis et al., 1979; Düzgüneş & Papahadjopoulos, 1983). Our work implies that if this proposal is correct, then the extent of dehydration between the bilayers must also follow the sequence $Ca^{2+} > Ba^{2+} > Sr^{2+} > Mg^{2+}$.

It is still an open question as to whether these new binding complexes will provide a unified description of fusion, lateral phase separation, and thermometric behavior of the bilayers. Our analysis provides the initial amounts of bound divalent cations needed to induce threshold fusion rates but cannot specify which types of cation/phospholipid complexes will cause the fusion. If the destabilization does require a critical density of these new binding complexes between the apposed bilayers, then the rate of destabilization will be determined by the initial amount of bound divalent cation, by the diffusion of these bound divalent cations into the area of contact, and

Table III: Binding Constants for Na^+, Ca^{2+}, and Mg^{2+} to PS[a]

set	K_1(Na)	K_2^+(Ca)	K_2^0(Ca)	K_2^+(Mg)	K_2^0(Mg)	ref
1	0.6	12	0	8	0	McLaughlin et al. (1981)
2	0.8	0	35	0	20	Nir et al. (1978) and Portis et al. (1979)
3	0.6	0	30	0	10	Ohki & Kurland (1981)

[a] All of these binding constants have the units of M^{-1}. The values of McLaughlin et al. (1981) (set 1) were obtained from the electrophoretic mobilities of large PS MLV by assuming that all of the cations bound 1:1 to the PS head groups. The values of Nir et al. (1978) and Portis et al. (1979) (set 2) were obtained from equilibrium dialysis and atomic absorption spectroscopy of PS SUV by assuming that each Ca^{2+} or Mg^{2+} bound to two adjacent PS head groups. The values of Ohki & Kurland (1981) (set 3) were obtained from surface potential changes of PS monolayers on an air–water interface by assuming that the divalent cations bound to two adjacent PS head groups.

Table IV: Calculated Amounts of Bound Divalent Cations for the Sets of Binding Constants Given in Table III for PS SUV[a]

$[Na^+]$ (mM)	$[Ca^{2+}]$ (mM)	Ca bound per PS		
		calcn 1	calcn 2	calcn 3
100	1	0.293	0.302	0.309
	5	0.380	0.376	0.378
300	1	0.151	0.160	0.175
	5	0.276	0.287	0.296
500	1	0.090	0.095	0.109
	5	0.211	0.223	0.236
900	2	0.074	0.079	0.090
$[Na^+]$ (mM)	$[Mg^{2+}]$ (mM)	Mg bound per PS		
		calcn 1	calcn 2	calcn 3
100	1	0.265	0.264	0.236
	5	0.359	0.350	0.325
300	1	0.121	0.117	0.095
	5	0.244	0.243	0.212
500	1	0.068	0.063	0.048
	5	0.177	0.175	0.145

[a] These values are calculated from the equations given in Bentz (1981, 1982) by using the following parameters: radius of vesicle = 150 Å; area per head group = 70 Å^2; temperature = 20 °C. The binding constants used in calculations 1–3 were taken from sets 1–3, respectively, of Table III. Equivalent calculations using Li^+ instead of Na^+ show the same degree of agreement between the three sets of binding constants. On the other hand, it is important to recognize that the other calculated parameters, e.g., surface potential (Ψ_0), show greater sensitivity to the particular set of binding constants used.

by the rate of formation of the new interbilayer complexes. This study proves that less Ca^{2+}, than Ba^{2+} or Sr^{2+}, is needed initially to produce the same rate of destabilization. Further studies are needed to establish whether fewer Ca^{2+} complexes are necessary to destabilize the bilayers or whether they simply form more rapidly.

Conclusions

The analysis of fusion kinetics presented elsewhere for general cases (Bentz et al., 1983) and in the simplified form given here for those cases where the aggregation rate is modified to very large values has considerably simplified the conceptual picture of fusion. In particular, the fusion process is shown to follow straightforward mass action kinetics. Thus, we can deduce the values of aggregation rate constants, which are precise measures of the interaction energies between the vesicles, and the values of fusion rate constants, which are precise measures of the destabilization step between two apposed membranes. This kinetic analysis provides a single format by which the capacities of the mono- and divalent cations to bind to, to aggregate, and to fuse these vesicles can be analyzed. This analysis is appropriate for a wide variety of vesicle systems and for any fusion assay which can be directly related to the number of fused vesicles. Our quantitative analysis of divalent cation induced fusion supports previous proposals that they share a common mechanism for fusion but that each cation has a different capacity to activate this mechanism (Liao & Prestegard, 1980b; Ohki, 1982). While the molecular basis of the mechanism is still a speculative issue, this work clearly establishes new and rigorous criteria which any proposed mechanism must satisfy.

Acknowledgments

We thank Andrea Mazel for the expert typing of the manuscript. The experimental work was performed in the laboratory of Dr. D. Papahadjopoulos.

Appendix

The analysis and prediction of the amounts of cations bound to membranes made of acidic phospholipids are an ongoing problem [see Nir et al. (1983) for a review]. Binding of the cations to the head groups of molecules comprising the bilayers is established, but the details of this process are still being resolved. In this appendix, we only consider the binding of the cations to an isolated membrane surface. There are currently two ways of expressing the binding of divalent cations to these head groups: either the divalent cation is presumed to bind to a single head group [1:1 stoichiometry; e.g., see McLaughlin et al. (1981)] or it is presumed to bind to two adjacent headgroups [2:1 stoichiometry; e.g., see Nir et al. (1978) and Ohki & Kurland (1981)]. Since the choice of the binding stoichiometry will prescribe the measured values of the binding constants and since we are interested in how the onset of bilayer destabilization depends on the amount of bound divalent cation, it is important to know that these different binding models and constants yield the same values for the amount of bound divalent cation. We show here that this is indeed the case. On the other hand, the remaining parameters of cation binding (e.g., surface potentials and amounts of bound monovalent cations) are dependent upon the specific binding model.

The binding of the cations to the PS head groups is assumed to follow a simple mass action equilibrium at the bilayer surface. In Table III, we list the binding constants for Na^+, Ca^{2+}, and Mg^{2+} to PS head groups as determined by several studies. We have included only those studies which simultaneously accounted for the competition between cations in the electrolyte for binding sites and the accumulation of cations near the charged PS surfaces. Neglecting the latter effect in order to measure so-called "apparent" binding constants for PS vesicles or monolayers has been shown to yield unreliable results (Bentz & Nir, 1980). The binding constant for Ca^{2+} is denoted by K_2^+(Ca) for the studies which presumed that Ca^{2+} binds to a single head group, thereby yielding a Ca/PS^+ complex. For the other studies which presumed that Ca^{2+} binds to two adjacent PS head groups, yielding a neutral Ca/PS_2 complex, we have denoted the binding constant as K_2^0(Ca). The same notation is used for Mg^{2+}. All the studies presumed that Na^+ competed for one PS head group binding site. McLaughlin et al. (1981) have proven the existence of the 1:1 binding stoichiometry for the divalent cations by showing that large multilamellar vesicles could reverse the sign

of their surface potentials in high concentrations of divalent cation; however, this study could not exclude the simultaneous existence of the 2:1 binding mode.

Given any set of binding constants, we can calculate the amount of divalent cation bound per PS head group for SUV by solving the Poisson–Boltzmann equation. Recently, we have developed a simple and accurate approximate solution for this problem for vesicles whose radius is too small to permit the use of the flat-plate assumption (Bentz, 1981, 1982). Table IV shows the predicted amounts of bound Ca^{2+} or Mg^{2+} per PS as a function of different electrolyte compositions.

Several comments are necessary to clarify the limitations to these calculations. Measurements of bound Ca^{2+} to PS SUV in the presence of 100–500 mM Na^+ (where there was not significant fusion) were predicted quite well by using the values of set 2 of Table III (Düzgüneş et al., 1981a). However, the same study showed an underestimate of the bound Ca^{2+} in 1000 mM Na^+: a result we attribute to the aggregation of the vesicles and the emergence of the new binding complexes since the vesicles were dialyzed for 6 h and we know that slow fusion occurs in this system. Hence, these calculations give good estimates for the amounts of bound divalent cations in the range of 100–500 mM Na^+ before the vesicles begin to aggregate and fuse. Eisenberg et al. (1979) showed that microelectrophoresis of the PS MLV in 3–100 mM Na^+ was well predicted by using 0.6 M^{-1} for the Na^+ binding constant; however, McLaughlin et al. (1981) noted that in 10 mM Na^+ the 1:1 binding constant of Ca^{2+} appeared to be 3-fold higher than the value obtained in 100 mM Na^+ shown in set 1 of Table III. This result implies that the binding of Ca^{2+} at low Na^+ concentrations is not straightforward. In Figure 3, we did not attempt to correct the calculations for this effect in 20 and 50 mM Na^+. However, it is clear that such a correction would only increase the separation between the high and low Na^+ concentration curves in Figure 3c.

Finally, Cohen & Cohen (1981) have shown that the data generated by the studies cited in Table III could be fitted by assuming that the monovalent cations bind to different sites on the PS head group than do the divalent cations; i.e., there is noncompetitive binding of cations. This speculation is interesting; however, there has been no experimental verification. We analyzed their model, by using the electrolytes given in Table IV, with the binding constants of McLaughlin et al. (1981), since these binding constants would remain essentially unchanged regardless of whether the binding is competitive or not. Surprisingly, the calculated amounts of bound divalent cations never varied from the amounts shown in column 1 of Table IV by more than 0.04, the greatest deviation occurring with high Na^+ and low Ca^{2+} or Mg^{2+} concentrations. In 500 mM Na^+ with 5 mM Ca^{2+} or Mg^{2+}, which is the relevant regime for the fusion threshold, the noncompetitive model yielded 0.226 and 0.198 divalent cation bound per PS, respectively. Such differences are clearly within the experimental error of the measurements.

Taken together, these results show that our estimates for the amounts of bound divalent cation used in Figure 4 and Table I do not vary significantly regardless of which binding model is chosen to make the calculations. For Ca^{2+}, it is evident that all three sets of binding constants give essentially the same values. For Mg^{2+}, the values predicted from Ohki & Kurland (1981) are somewhat smaller. Insofar as the experimental studies used different techniques to measure the cation binding, the concordance of the results is good. Given that we are comparing the four divalent cations and the two monovalent cations, we prefer to use the binding constants of Eisenberg et al. (1979) and McLaughlin et al. (1981) because they were all obtained from the same experimental technique—microelectrophoresis of PS MLV. Thus, if there are any systematic differences between the different experimental techniques and systems, this would only affect the numerical estimates of the threshold amounts of bound divalent cations needed to induce fusion, without affecting the sequence of their fusogenic capacities.

Registry No. Ba, 7440-39-3; Ca, 7440-70-2; Sr, 7440-24-6; Mg, 7439-95-4.

References

Bartlett, G. R. (1959) *J. Biol. Chem. 234*, 466–468.

Bentz, J. (1981) *J. Colloid Interface Sci. 80*, 179–191.

Bentz, J. (1982) *J. Colloid Interface Sci. 90*, 164–182.

Bentz, J., & Nir, S. (1980) *Bull. Math. Biol. 42*, 191–220.

Bentz, J., & Nir, S. (1981a) *Proc. Natl. Acad. Sci. U.S.A. 78*, 1634–1637.

Bentz, J., & Nir, S. (1981b) *J. Chem. Soc., Faraday Trans. 1 77*, 1249–1275.

Bentz, J., Nir, S., & Wilschut, J. (1983) *Colloids and Surfaces* (in press).

Cohen, J. A., & Cohen, M. (1981) *Biophys. J. 36*, 623–651.

Düzgüneş, N., & Papahadjopoulos, D. (1983) in *Membrane Fluidity in Biology: General Principles* (Aloia, R. C., Ed.) Vol. 2, Academic Press, New York (in press).

Düzgüneş, N., Nir, S., Wilschut, J., Bentz, J., Newton, C., Portis, A., & Papahadjopoulos, D. (1981a) *J. Membr. Biol. 59*, 115–125.

Düzgüneş, N., Wilschut, J., Fraley, R., & Papahadjopoulos, D. (1981b) *Biochim. Biophys. Acta 642*, 182–195.

Düzgüneş, N., Rehfeld, S. J., Freeman, K. B., Newton, C., Eatough, D. J., & Papahadjopoulos, D. (1981c) Abstracts of the VIIth International Biophysics Congress, Mexico City, Mexico, p 226.

Düzgüneş, N., Bentz, J., Freeman, K., Nir, S., & Papahadjopoulos, D. (1983a) *Fed. Proc., Fed. Am. Soc. Exp. Biol. 42*, 1771.

Düzgüneş, N., Paiement, J., Freeman, K., Lopez, N., Wilschut, J., & Papahadjopoulos, D. (1983b) *Biophys. J. 41*, 30a.

Eisenberg, M., Gresalfi, T., Riccio, T., & McLaughlin, S. (1979) *Biochemistry 18*, 5213–5223.

Ekerdt, R., & Papahadjopoulos, D. (1982) *Proc. Natl. Acad. Sci. U.S.A. 79*, 2273–2277.

Hammoudah, M. M., Nir, S., Bentz, J., Mayhew, E., Stewart, T. P., Hui, S. W., & Kurland, R. J. (1981) *Biochim. Biophys. Acta 645*, 102–114.

Hoekstra, D. (1982a) *Biochemistry 21*, 1055–1061.

Hoekstra, D. (1982b) *Biochemistry 21*, 2833–2840.

Hoekstra, D., Yaron, A., Carmel, A., & Scherphof, G. (1979) *FEBS Lett. 106*, 176–180.

Kerker, M. (1969) *The Scattering of Light and Other Electromagnetic Radiation*, Academic Press, New York.

Kurland, R., Newton, C., Nir, S., & Papahadjopoulos, D. (1979) *Biochim. Biophys. Acta 551*, 137–147.

Liao, M.-J., & Prestegard, J. H. (1980a) *Biochim. Biophys. Acta 599*, 81–94.

Liao, M.-J., & Prestegard, J. H. (1980b) *Biochim. Biophys. Acta 601*, 453–461.

McLaughlin, S., Mulrine, N., Gresalfi, T., Vaio, G., & McLaughlin, A. (1981) *J. Gen. Physiol. 77*, 445–473.

Miller, D. C., & Dahl, G. P. (1982) *Biochim. Biophys. Acta 689*, 165–169.

Newton, C., Pangborn, W., Nir, S., & Papahadjopoulos, D. (1978) *Biochim. Biophys. Acta 506*, 281–287.

Nir, S., & Bentz, J. (1978) *J. Colloid Interface Sci. 65*, 399–414.

Nir, S., Newton, C., & Papahadjopoulos, D. (1978) *Bioelectrochem. Bioenerg. 5*, 116–133.
Nir, S., Bentz, J., & Portis, A. (1980a) *Adv. Chem. Ser. No. 188*, 75–106.
Nir, S., Bentz, J., & Wilschut, J. (1980b) *Biochemistry 19*, 6030–6036.
Nir, S., Bentz, J., & Düzgüneş, N. (1981) *J. Colloid Interface Sci. 84*, 266–269.
Nir, S., Wilschut, J., & Bentz, J. (1982) *Biochim. Biophys. Acta 688*, 275–278.
Nir, S., Bentz, J., Wilschut, J., & Düzgüneş, N. (1983) *Prog. Surf. Sci. 13*, 1–124.
Ohki, S. (1982) *Biochim. Biophys. Acta 689*, 1–11.
Ohki, S., & Düzgüneş, N. (1979) *Biochim. Biophys. Acta 552*, 438–449.
Ohki, S., & Kurland, R. (1981) *Biochim. Biophys. Acta 645*, 170–176.
Ohki, S., Düzgüneş, N., & Leonards, K. (1982) *Biochemistry 21*, 2127–2133.
Ohnishi, S. I., & Ito, T. (1974) *Biochemistry 13*, 881–887.
Papahadjopoulos, D., Poste, G., Schaeffer, B. E., & Vail, W. J. (1974) *Biochim. Biophys. Acta 352*, 10–28.
Papahadjopoulos, D., Vail, W. J., Jacobson, K., & Poste, G. (1975) *Biochim. Biophys. Acta 394*, 483–491.
Papahadjopoulos, D., Vail, W. J., Pangborn, W. A., & Poste, G. (1976) *Biochim. Biophys. Acta 448*, 265–283.
Portis, A., Newton, C., Pangborn, W., & Papahadjopoulos, D. (1979) *Biochemistry 18*, 780–790.
Rehfeld, S. J., Düzgüneş, N., Newton, C., Papahadjopoulos, D., & Eatough, D. J. (1981) *FEBS Lett. 123*, 249–251.
Schmidt, C. F., Lichtenberg, D., & Thompson, T. E. (1981) *Biochemistry 20*, 4792–4797.
Schullery, S. E., Schmidt, C. F., Felgner, P., Tillack, T. W., & Thompson, T. E. (1980) *Biochemistry 19*, 3919–3923.
Struck, D., Hoekstra, D., & Pagano, R. E. (1981) *Biochemistry 20*, 4093–4099.
Sundler, R., & Papahadjopoulos, D. (1981) *Biochim. Biophys. Acta 649*, 743–750.
Vistnes, A. I., & Puskin, J. S. (1981) *Biochim. Biophys. Acta 644*, 244–250.
Wilschut, J., & Papahadjopoulos, D. (1979) *Nature (London) 281*, 690–692.
Wilschut, J., Düzgüneş, N., Fraley, R., & Papahadjopoulos, D. (1980) *Biochemistry 19*, 6011–6021.
Wilschut, J., Düzgüneş, N., & Papahadjopoulos, D. (1981) *Biochemistry 20*, 3126–3133.
Wong, M., & Thompson, T. E. (1982) *Biochemistry 21*, 4133–4139.
Wong, M., Anthony, F. H., Tillack, T. W., & Thompson, T. E. (1982) *Biochemistry 21*, 4126–4132.

Circular Dichroism and Fluorescence Studies on a Cation Channel Forming Plasma Membrane Proteolipid†

Victor S. Sapirstein* and Thomas C. Rounds

ABSTRACT: The structure of a plasma membrane proteolipid complex that forms a voltage-dependent cation channel was probed by using circular dichroism and fluorescence in water, in liposomes, and in organic solvents. The protein in water exhibited one peak of tryptophan emission at 335 nm, suggesting that in water this amino acid is restricted to a hydrophobic environment. In chloroform–methanol and in liposomes, the spectrum had emission maxima at 345 nm as well as at 335 nm. These data suggest that in chloroform–methanol or after introduction into liposomes the protein undergoes a conformational shift from the water-soluble form; some or all of the tryptophan residues (or a population of tryptophan residues of the proteolipid) appear to be shifted to a more hydrophilic environment. Analysis of the extrinsic fluorescence obtained through energy transfer to 8-anilino-1-naphthalenesulfonate suggests that the proteolipid complex exists in different states of oligomerization in organic solvents and in water. Circular dichroism studies of the water-soluble form indicated that the protein is 73% α helix, 14% β structure, and 12% random coil, indicative of the presence of a large hydrophobic interior. Addition of sodium dodecyl sulfate to the proteolipid in water did not greatly reduce the percent α helix and only slightly decreased the contribution of β structure, suggesting that sodium dodecyl sulfate has little access to the helix-forming hydrophobic interior. Trifluoroethanol induced a predictable increase in the helical content. Most significant was the change in secondary structure after introduction of the protein into phosphatidylcholine–cholesterol liposomes; a small reduction in helical content was accompanied by an almost total elimination of β structure with a concomitant increase to 35% of the contribution by the random structure.

Proteolipids are a class of hydrophobic membrane proteins characterized by their solubility in chloroform–methanol (Lees et al., 1979; Schlesinger, 1981). The delipidated apoproteins retain their solubility in chloroform–methanol but can be converted to water-soluble forms by several methods (Lees & Sakura, 1978; Cockle et al., 1978a). Proteolipid proteins were first described in central nervous system myelin (Folch & Lees, 1951) where the proteolipid accounts for 50% of the total protein; since then, different proteolipids have been isolated from mitochodria (Beechey et al., 1975; Enna & Criddle, 1977; Sebald & Wachter, 1978), sarcoplasmic reticulum (Maclennan et al., 1973; Eytan & Racker, 1977), and plasma membranes (Tosteson & Sapirstein, 1981). Although the proteolipids from these different membranes are distinct, they do share certain characteristics in addition to their solubility properties. The myelin (Ting-Beall et al., 1979), mitochondrial (Miller & Racker, 1976), sarcoplasmic reticulum (Racker & Eytan, 1975), and plasma membrane proteolipids (Tosteson & Sa-

† From the Department of Biochemistry, Eunice Kennedy Shriver Center for Mental Retardation, Inc., Waltham, Massachusetts 02254, and the Department of Biological Chemistry, Harvard Medical School, Boston, Massachusetts 02115. *Received September 28, 1982; revised manuscript received April 4, 1983.* This work was supported by National Institutes of Health Grants NS16186, HD05515, and AM07300.

* Address correspondence to this author at the Department of Biochemistry, Eunice Kennedy Shriver Center for Mental Retardation, Inc.

0006-2960/83/0422-3330$01.50/0 © 1983 American Chemical Society